µFLU12-156

EFFECT OF CHANNEL SHAPE ON AXIAL BACK CONDUCTION IN THE SOLID SUBSTRATE OF MICROCHANNELS

Manoj Kumar Moharana*[1], Sameer Khandekar[2]

[1]Department of Mechanical Engineering
National Institute of Technology Rourkela, Rourkela 769008 (Odisha) India
moharanam@nitrkl.ac.in

[2]Department of Mechanical Engineering
Indian Institute of Technology Kanpur, Kanpur 208016 (U.P) India
samkhan@iitk.ac.in

KEY WORDS

Simultaneously developing internal convective flows in rectangular microchannels, Conjugate heat transfer, Axial heat conduction in the substrate, Optimum Nusselt number.

ABSTRACT

Microchannels machined on flat solid substrates (metallic/non-metallic) are widely used in many engineering heat transfer applications. Such applications, on most occasions, involve conjugate effects, overlooking of which often leads to misinterpretation of transfer coefficients. In this background, a conjugate three-dimensional numerical simulation of simultaneously developing laminar flow in rectangular microchannels has been carried out. A substrate of fixed size (0.6 mm × 0.4 mm × 60 mm) is considered while the channel width and height are independently varied such that the channel aspect ratio varies from 1.0 to 4.0 to find the effect of microchannel aspect ratio on axial back conduction. Considering the fact that axial conduction dominates at low flow rates, the flow Reynolds number of the working fluid considered is 100. The thermal conductivity of the solid substrate as well as the working fluid are considered in the conjugate formulation. Constant heat flux is applied at the bottom of the substrate while all its other surfaces are kept insulated. Detailed parametric study reveals that depending on channel aspect ratio and thermo-physical properties of fluid-solid combination, conjugate heat transfer effects must be accounted for, to correctly estimate the local Nusselt number along the channel. The average Nusselt number is found to be minimum corresponding to channel aspect ratio of 2.0, irrespective of the conductivity ratio of the solid substrate and the working fluid.

1. INTRODUCTION

In conventional size channels under fully developed flow conditions in a duct/channel, a constant heat flux boundary condition at the solid-fluid interface leads to maximum heat transfer coefficient. In many engineering applications a situation with constant heat flux on one, or some of the surfaces being heated, arises. While the objective ought to be to have the constant heat flux exactly at the solid-fluid interface, in reality, for several practical limitations, the surface on which the constant heat flux is actually applied is at a certain finite distance from the true solid-fluid interface. This leads to multi-dimensional conjugate heat transfer, depending on several factors, viz., the geometric configuration of the solid and fluid domain, thermo-physical properties of the solid substrate and fluid involved, and flow conditions. In some cases it is likely that the effective thermal resistance in the solid medium in the axial direction is such that heat actually flows by conduction in the solid substrate in the axial direction, opposite to the streamwise direction. This

---

* Corresponding author

phenomena of 'axial back conduction', distorts the true boundary condition of constant heat flux at the solid-fluid interface. This, in turn, reduces heat transfer coefficient. The effect of axial conduction gets magnified in microchannel systems and likely to give inaccurate heat transfer coefficient estimation, if over-looked

The study of axial conduction in the solid domain in a convective heat transport system was carried out as early as in 1964, by Bahnke and Howard [1]. Later on Petukhov [2] studied axial conduction in the solid wall of a circular tube using a parameter which is function of thermal conductivity ratio of the solid walls and the working fluid, and the tube thickness to inner radius ratio. Other similar studies were done by Faghri and Sparrow [3], Chiou et al. [4], and Cotton and Jackson [5]. Though the study on axial conduction continued with time, the number of studies are quiet few. The study on axial conduction again gained momentum with development of microscale heat transfer devices. This is because of relative importance of axial conduction effect in such small geometries, as compared to heat transfer applications employing conventional sized channels. Peterson [6] numerically studied conduction effects in microscale counter flow heat exchangers. Maranzana et al. [7] introduced a number called axial conduction number (M) which is defined as the ratio of the conductive heat flux to the convective counterpart. Maranzana et al. [7] also stated that axial conduction in the solid substrate will be negligible if M < 0.01. Li et al. [8] and Zhang et al. [9], based on their study on conjugate heat transfer in thick circular tubes concluded that the criterion for neglecting axial conduction as proposed by Maranzana et al. [7] may not be always valid. They stated that depending on the boundary conditions and geometrical parameters the criteria for judging the effect of axial wall conduction may vary on case to case basis.

Recently Moharana et al. [10] carried out numerical analysis of axial conduction in a circular micro tube and a square shaped microchannel on a solid substrate, considering wide parametric variations. Their study suggests that for both the microtube as well as square microchannel on solid substrate, there exists an optimum value of conductivity ratio (conductivity of the solid substrate material to conductivity of working fluid) which maximizes the average Nusselt number over the channel length. This observation was based on an extensive parametric variation of conductivity ratio, flow Re and substrate thickness, while the heating perimeter was kept constant i.e. a square channel of constant dimensions. This can be explained as follows: Higher conductivity ratio leads to severe axial back conduction, thus decreases average Nu. Very low value of conductivity ratio leads to a situation which is qualitatively similar to the case of zero thickness substrate with constant heat flux applied on one wall only (the other three sides being adiabatic). This again lowers the average value of Nu. A very close observation to understand this phenomenon revealed that with decreasing conductivity ratio, the thermal resistance to flow of heat to the two vertical walls of the square channel increases. From this observation it is expected that while all other factors remaining the same, the channel aspect ratio will also play a major role in the conjugate heat transfer process.

In this background, we have conducted a three-dimensional numerical investigation, using commercially available Ansys-Fluent®, to understand and highlight the effect of channel aspect ratio (ratio of channel width to the channel height) on the axial wall conduction in a steady-state laminar incompressible simultaneously developing flow and ensuing heat transfer in rectangular microchannels. Considering extensive use of rectangular microchannels for a variety of practical applications, we consider the system as shown schematically in Figure 1. A uniform wall heat flux applied at the bottom of the substrate with all other surfaces being insulated is modeled, as shown. Thermophysical properties of both the solid and the fluid domain are assumed to be constant. Peripherally averaged (over three heating sides) local heat flux, wall temperature and average bulk fluid temperature are numerically calculated as functions of the dimensionless axial distance, channel aspect ratio, and thermal conductivity ratio of solid to fluid. Simulations have been carried out for a wide range of substrate wall to fluid conductivity ratio (12.2 - 635), channel aspect ratio (1.0 - 4.0) for a fixed substrate dimension. A low flow rate case (Re = 100) has been reported here, as it represents a typical case, prone to the effects of axial conduction. These parametric variations cover the typical range of applications encountered in micro-fluids/micro-scale heat transfer domains. To discern the explicit effect of channel aspect ratio and the heating perimeter, we conduct two types of simulations: (i) First, the channel aspect ratio is varied such that the area of cross-section of the channel is constant. (ii) Secondly, the channel aspect ratio is again varied such that the heating perimeter of the channel is constant. Peripherally averaged local heat flux, wall temperature and average bulk fluid temperature are numerically calculated as functions of the dimensionless axial distance, channel aspect ratio, and thermal conductivity ratio of solid to fluid. Extensive grid independence and validation of the numerical scheme is done before carrying out the simulations reported here.
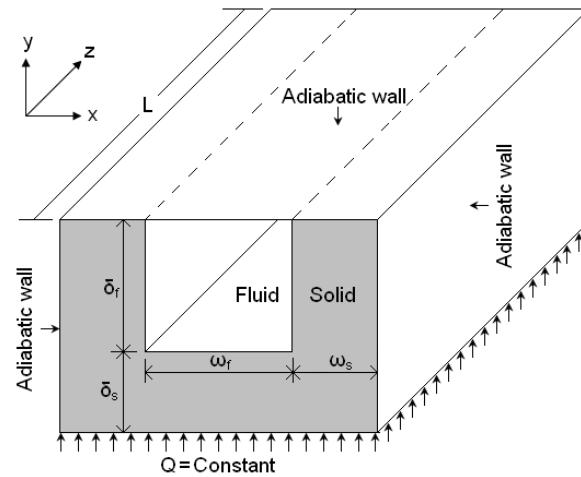
Figure 1: Microchannel in a solid substrate.

2. NUMERICAL ANALYSIS

In the present investigation it is assumed that the heat transfer and fluid flow takes place at steady state, the flow is laminar, incompressible with constant thermo-physical properties and the amount of heat loss either by radiation or by means of natural convection is negligible. Again referring to Figure 1, the width $(2 \cdot \omega_s + \omega_f)$, the thickness $(\delta_s + \delta_f)$, and the length (L) of the substrate are kept constant in the computational model at 0.6 mm, 0.4 mm, and 60 mm respectively. The aspect ratio of the channel in which the fluid is flowing is varied, i.e., by varying the channel width (ω_f), and the channel height (δ_f); thus, the hydraulic diameter (D_h) of the channel ranges from 0.16 - 0.203 mm**.** In actual computations, only one half of this section, along the vertical plane of symmetry, was considered. As discussed earlier, a constant heat flux boundary condition is applied at bottom of the substrate and all other outer surfaces are insulated, as shown in Figure 1. Coupled equations for conservation of mass, momentum and energy are solved on this domain using commercial platform Ansys-Fluent[®]. The multi-grid solution procedure incorporates the standard scheme for pressure discretization and the SIMPLE algorithm for velocity-pressure coupling. Momentum and energy equations are solved using the 2ⁿᵈ order upwind scheme. Water is used as the working fluid, which enters the microchannel with a uniform 1-D velocity profile, at an inlet temperature of 300K. Thus, the flow is hydrodynamically as well as thermally developing in nature during its transit in the channel.
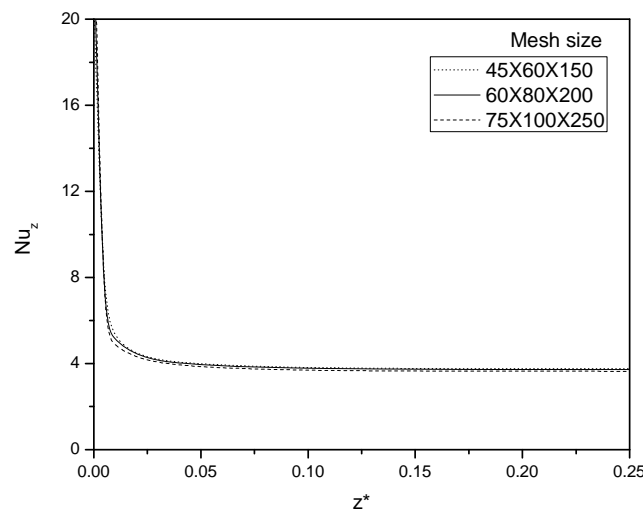
Figure 2: Grid independence check: Variation of local Nusselt number calculated along the streamwise direction for the channel size of 0.4 mm × 0.4 mm × 60 mm, with $\delta_{sf} = 1$, and three mesh sizes.

The computational domain was meshed using hexahedral elements and the grid independence was ensured before deciding the grid size for each case under consideration. For an example, local Nusselt number calculated for a substrate with $\delta_{sf} = 1$ (δ_{sf} is defined as the ratio of δ_s and δ_f , where δ_s is the thickness of the

solid substrate below the channel, and δ_f is defined as the height of the channel) for three mesh sizes of $45\times60\times150$, $60\times80\times200$ and $75\times100\times250$ (for half of the geometry as shown in Figure 1.), for Re = 100, is as shown in Figure 2. The peripheral averaged local Nusselt number at the fully developed flow regime near the channel outlet changed by 1.06% from the mesh size of $45\times60\times150$ to $60\times80\times200$, and changed by less than 1% on further refinement to mesh size of $75\times100\times250$. As we moved from first to the third mesh, no appreciable change is observed. So, the intermediate grid ($60\times80\times200$) was selected, which corresponds to actual physical average spacing of 0.01 mm along the width and height (x and y axis) and 0.3 mm along the channel length (z axis). Finer meshing was used in the channel entrance and the boundary layers.

3. DATA REDUCTION

The microchannel hydraulic diameter (D_h), channel aspect ratio (ε), conductivity ratio (k_{sf}), cross sectional area ratio (A_{sf}) are defined (with reference to Fig. 1) as follows:

$$A_f = \omega_f \cdot \delta_f, \quad A_s = (\omega_f + 2\omega_s)(\delta_s + \delta_f) - A_f, \tag{1}$$

$$D_h = \frac{2A_f}{\delta_f + \omega_f}, \quad \varepsilon = \frac{\omega_f}{\delta_f}, \quad k_{sf} = \frac{k_s}{k_f}, \quad A_{sf} = \frac{A_s}{A_f}, \tag{2}$$

where ω_f = channel width, δ_f = channel height, ω_s = width of channel vertical wall, δ_s = thickness of channel horizontal wall i.e. substrate thickness below channel bottom wall, k_s = thermal conductivity of the solid substrate, k_f = thermal conductivity of the working fluid, A_s = Area of cross section of the solid substrate, A_f = area of cross section of channel. The heating perimeter (P_h) is defined as the perimeter of the conjugate walls of the channel, is represented as

$$P_h = \omega_f + 2\delta_f, \tag{3}$$

The axial coordinate, z, is non-dimensionalized as:

$$z^* = z/L, \tag{4}$$

where L = length of the channel. The applied heat flux at the bottom of the substrate is defined as follows:

$$\overline{q}'_{applied} = \frac{Q}{(2 \cdot \omega_s + \omega_f)L}, \tag{5}$$

where, Q is the heat input to the bottom of the substrate. The ideal heat flux at the solid fluid interface is given by:

$$\overline{q}' = \overline{q}'_{applied} \frac{(2 \cdot \omega_s + \omega_f)}{(2 \cdot \delta_f + \omega_f)}, \tag{6}$$

The non-dimensional local heat flux at the fluid-solid interface is given by:

$$\phi = q'_z / \overline{q}', \tag{7}$$

where q'_z is the peripheral averaged local heat flux transferred at the solid-fluid interface along the channel length (only the three heating sides are included for calculating this peripheral average value, as the top wall is adiabatic). The dimensionless bulk fluid and channel wall temperatures are given by:

$$\Theta_f = \frac{\overline{T}_f - \overline{T}_{fi}}{\overline{\overline{T}}_{fo} - \overline{\overline{T}}_{fi}}, \tag{8}$$

$$\Theta_w = \frac{\overline{T}_w - \overline{T}_{fi}}{\overline{\overline{T}}_{fo} - \overline{\overline{T}}_{fi}}, \tag{9}$$

where $\overline{T}_{fi}$ and $\overline{T}_{fo}$ are the average bulk fluid temperature at the channel inlet and outlet respectively; $\overline{T}_f$ is the average bulk fluid temperature at any location and $\overline{T}_w$ is the peripheral average wall temperature at the same location (here too, only three heating sides are included to calculate the peripheral average wall temperature). The local Nusselt number is then given by:

$$Nu_z = h_z \cdot D_h / k_f, \tag{10}$$

where the local heat transfer coefficient is given by:

$$h_z = \frac{q'_z}{(\overline{T}_w - \overline{T}_f)}, \tag{11}$$

The average Nusselt number over the whole channel length is given by:

$$\overline{Nu} = \int_{z=0}^{L} Nu_z dz, \tag{12}$$

MICROFLUIDICS2012

Proceedings of the 3rd European Conference on Microfluidics - Microfluidics 2012 - Heidelberg, December 3-5, 2012

4. RESULTS AND DISCUSSION

The size of the substrate is fixed (0.4 mm × 0.6 mm × 60 mm) while the channel aspect ratio is varied (ε ~ 1.0 – 4.0) to find the effect of channel aspect ratio on axial back conduction, and thereby the Nusselt number. The length of the channel is equal to the length of the substrate, and the hydraulic diameter of the channel ranges from 0.16 to 0.203 mm, depending on the channel aspect ratio. The channel aspect ratio is varied such that the area of cross-section of the channel is always constant (i.e. $\delta_f \cdot \omega_f$ = constant). Thus, the ratio of area of cross section of solid substrate to the channel, A_{sf} = 5.0 is constant. For each channel size, simulations have been performed for k_{sf} ~ 12.2 – 635. The working fluid used for all cases is water at inlet temperature of 300 K and flow Re = 100. Heat flux is applied on the bottom surface of the substrate which lies at a certain finite distance from the channel walls. Moreover, of the three conjugate walls of the channel, the channel bottom wall is parallel to the substrate bottom surface on which constant heat flux is applied, and the remaining two walls are perpendicular to the substrate bottom surface. The main parameters of interest are (a) peripheral average local heat flux (b) local bulk fluid temperature (c) peripheral average local wall temperature. These parameters allow us to determine the extent of axial conduction on the local Nu.

To find the magnitude of heat flux experienced at the conjugate walls of the rectangular channel, the axial variation of dimensionless heat flux, ϕ at the solid-fluid interface is presented in Figure 3. At very low conductivity ratio k_{sf} ($\approx$ 12.2), the actual heat flux experienced at the solid-fluid interface is approximately constant along the channel length. This can be observed in Figure 3 (a). At higher value of k_{sf} ($\approx$ 635), the heat flux experienced along the length of the channel substantially deviates from the ideal value of 1.0, especially at the inlet and the outlet region of the channel.
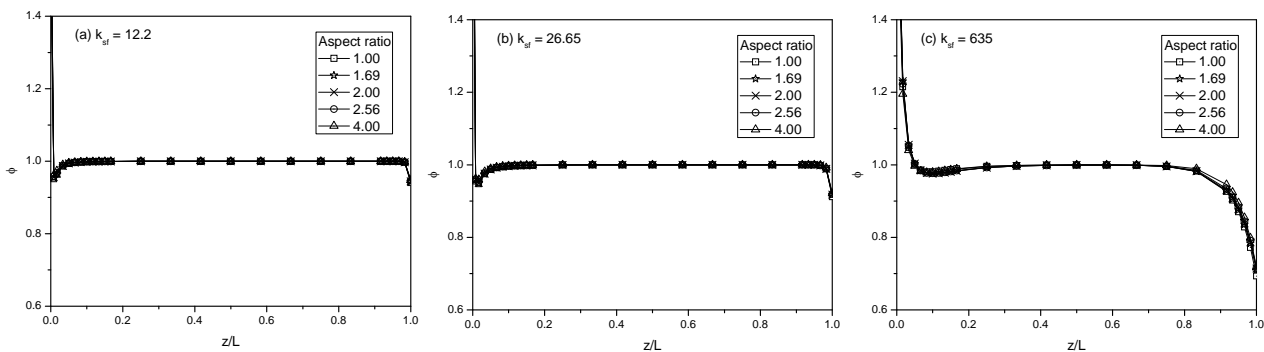
Figure 3: Variation of dimensionless local surface heat flux along the channel length.

Next, the axial variation of bulk fluid and channel wall temperature are explored, which are shown in Figure 4. Ideally, the fluid and the wall temperature varies linearly in the fully developed region. This trend is followed at lower k_{sf} ($\approx$ 12.2), which can be seen in Figure 4 (a). At higher k_{sf} ($\approx$ 635), the fluid and the wall temperature are deviating from linearity towards the end of the channel (see Figure 4 (c)). Secondly, the wall temperature at any axial location of the channel is found to be varying with channel aspect ratio irrespective of the value of k_{sf}, and the value of wall temperature is maximum when channel aspect ratio ε = 2.0. The bulk fluid temperature is independent of channel aspect ratio, ε.
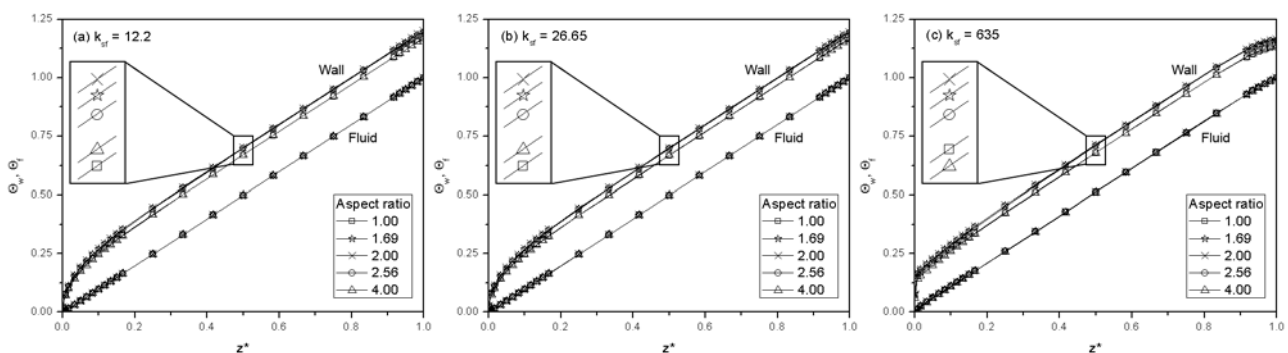
Figure 4: Variation of dimensionless local wall and local bulk fluid temperature along the channel length.

MICROFLUIDICS2012

Proceedings of the 3rd European Conference on Microfluidics - Microfluidics 2012 - Heidelberg, December 3-5, 2012

The axial variation of (a) heat flux at the solid-fluid interface, and (b) wall and bulk fluid temperatures will influence the behavior of the local Nusselt number along the channel length, as shown in Figure 5. Conventionally, the Nusselt number in the fully developed region is constant. This trend is followed at lower k_{sf} ($\approx$ 12.2), which can be seen in Figure 5 (a). At higher k_{sf} ($\approx$ 635), the Nusselt number does not remain constant towards the end of the channel (see Figure 5 (c)). Secondly, the Nusselt number at any axial location of the channel is found to be varying with channel aspect ratio irrespective of the value of k_{sf}, and the value of Nusselt number in the fully developed region is found to be minimum when the aspect ratio ε = 2.0.

From the above discussion it may be concluded that the channel aspect ratio also play some role in the heat transfer process, in addition to other parameters such as Re, k_{sf}, and substrate size. As discussed earlier Moharana et al. [10] had numerically studied effect of Re, k_{sf}, and substrate size on axial conduction; the present work is focused on role of channel aspect ratio. With varying channel height and width (i.e. channel aspect ratio), the channel heating perimeter ($P_h = 2 \cdot \delta_f + \omega_f$) also varies. The channel aspect ratio ε = 2.0 corresponds to minimum heating perimeter P_h. Based on the present study it may be concluded that minimum heating perimeter at ε = 2.0 leads to minimum local Nu_z in the fully developed region.
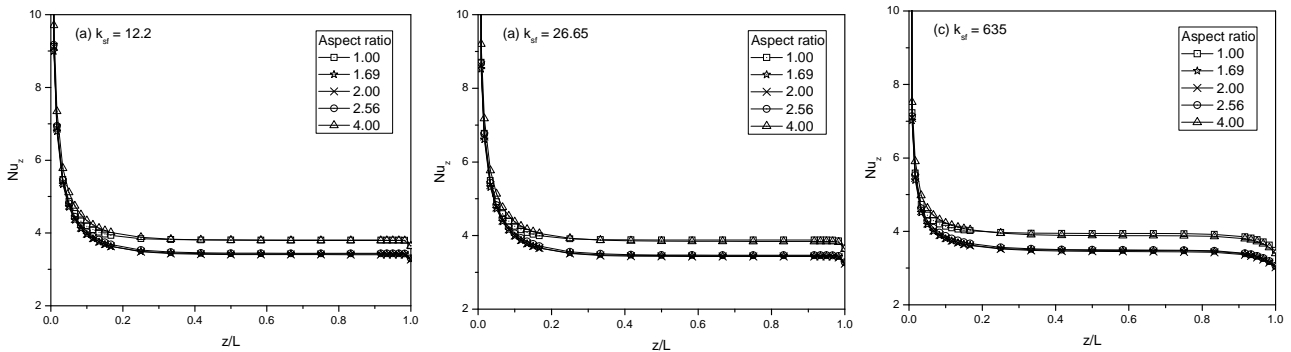
Figure 5: Variation of local Nusselt Number along the channel length.

In this background, the channel aspect ratio is again varied such that the heating perimeter (P_h) of the channel is constant. This makes total two cases: (i) the area of cross-section of the channel is constant (ii) the heating perimeter of the channel is constant. The variation of average Nusselt number ($\overline{Nu}$) over the whole channel length is plotted as function of conductivity ratio, k_{sf} as the channel aspect ratio ε is varied. This is shown in Figure 6. First, the occurrence of the optimum k_{sf} for maximizing the average Nusselt number is seen in Figure 6 (a) and (b) for every channel aspect ratio considered, which is inline with the previous study by Moharana et al. [10]. The prominent observation is that the magnitude of $\overline{Nu}$ is strong function of channel aspect ratio and is minimum at channel aspect ratio ε = 2.0. $\overline{Nu}$ increases with both increasing as well as decreasing channel aspect ratio away from ε = 2.0. It increases with both increasing as well as decreasing channel aspect ratio. For case (ii) also the results indicated that there exists a minima in the value of $\overline{Nu}$ at ε = 2.0 like the previous case though the heating perimeter (P_h) is constant unlike case (i).
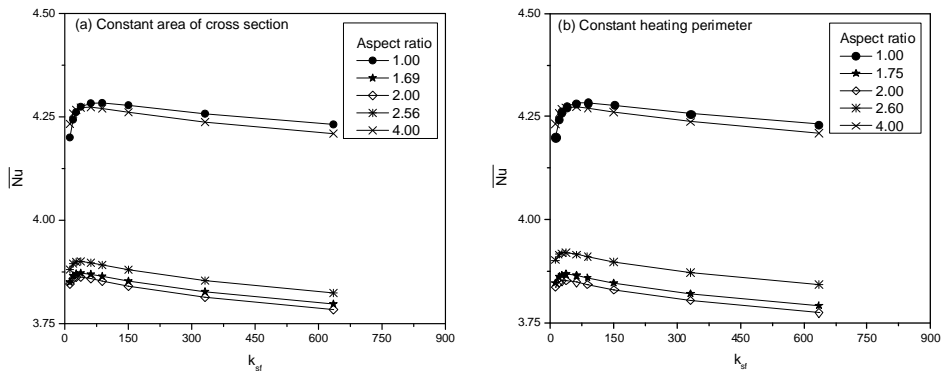
Figure 6: Variation of average Nusselt number of the rectangular microchannel with varying channel aspect ratio as a function of conductivity ratio, k_{sf} (a) constant area of channel cross section (b) constant channel heating perimeter.

For both the cases, the rate of increase of $\overline{Nu}$ with decrease in channel aspect ratio is more as compared to increase in channel aspect ratio. This observation is true irrespective of the value of conductivity ratio but

the value of conductivity ratio corresponding to peak value of average Nu is shifting to higher values with both increasing or decreasing channel aspect ratio i.e. the value of conductivity ratio corresponding to maximum average Nu is lowest when channel aspect ratio ε = 2.0. Recently Türkakar and Okutucu-Özyurt [11] studied dimensional optimization of rectangular silicon microchannel heat sinks and concluded that the thermal resistance decreases with increasing channel height (or decreasing channel aspect ratio). While this result is certainly in line with the results discussed above, the conclusions are only partly correct; Türkakar and Okutucu-Özyurt [11] did not capture the full spectrum of channel aspect ratio to observe presence of either maxima or minima. This is because their findings are based on a single value of conductivity ratio and only three values of channel aspect ratios.

5. SUMMARY AND CONCLUSIONS

In this work a three-dimensional numerical investigation is reported for flow through a rectangular microchannel on a solid substrate. A substrate of fixed size (0.4 mm × 0.6 mm × 60 mm) with varying channel aspect ratio ($\varepsilon \sim 1.0 - 4.0$) is used to find the effect of channel aspect ratio on axial back conduction. Heat flux is applied on the bottom surface of the substrate which lies at a certain finite distance from the channel walls. For each channel size, simulations have been performed for $k_{sf} \sim 12.2 - 635$. First, the channel aspect ratio is varied such that the area of cross-section of the channel is constant and A_{sf} = 5.0. The average Nusselt number over the length of the channel is found to be minimum when the channel aspect ratio is 2.0. Secondly, the channel aspect ratio is varied such that the heating perimeter is constant. For this case also the average Nusselt number over the length of the channel is found to be minimum when the channel aspect ratio is 2.0. For two different channel aspect ratio it is likely to lead to same value of average Nusselt number. In such a situation a microchannel with higher channel aspect ratio or lower channel depth is preferable considering that it is easy to manufacture channels with lower depth.

NOMENCLATURE

A_f cross-sectional area of channel i.e. fluid (-)
A_s cross-sectional area of solid substrate (-)
A_{sf} ratio of A_s and A_f (-)
C_p specific heat, J/kg-K
D_h hydraulic diameter, m
h   heat transfer coefficient, W/m²-k
k_f thermal conductivity of working fluid, W/m-K
k_s thermal conductivity of solid substrate, W/m-K
k_{sf} ratio of k_s and k_f (-)
L   length of the channel, m
Nu   Nusselt number (hD_h/k_f)
$\overline{Nu}$ average Nusselt number over the channel length
P_h heating perimeter (m)
Pr   Prandtl number ($C_p\mu/k_f$)
Q   total heat applied at the bottom of the substrate, W
$\overline{q}'$ average heat flux experienced at the channel walls, W/m²
$\overline{q}'_{applied}$ heat flux applied at the bottom of the substrate, W/m²
Re   Reynolds number ($\rho u D_h/\mu$)
T   temperature, K
$\overline{T}$ average temperature, K
z   axial coordinate
z*   non-dimensional axial distance along channel length (-)

Greek symbol

δ thickness, m
δ_f height of the channel, m
δ_s thickness of the solid substrate below the channel, m

δ_{sf} ratio of δ_s and δ_f (-)

ε channel aspect ratio (ω_f/δ_f) (-)

ω width, m

μ dynamic viscosity, Pa-s

ρ density, kg/m^3

ϕ non-dimensional local heat flux (-)

Θ non-dimensional temperature (-)

Subscript

f   fluid

i   inlet condition

o   outlet condition

s   solid

w   wall surface

z   axial length along the channel

ACKNOWLEDGEMENTS

REFERENCES AND CITATIONS

[1]   Bahnke, G. D., & Howard, C. P. (1964). The effect of longitudinal heat conduction on periodic-flow heat exchanger performance. *J. Eng. Power*, **86**, 105-120.

[2]   Petukhov, B. S. (1967). Heat transfer and drag of laminar flow of liquid in pipes. *Energiya*, Moscow.

[3]   Faghri, M., & Sparrow E. M. (1980). Simultaneous wall and fluid axial conduction in laminar pipe-flow heat transfer. *J. Heat Trans.*, **102**, 58-63.

[4]   Chiou, J. P. (1980). The advancement of compact heat exchanger theory considering the effects of longitudinal heat conduction and flow non-uniformity. symposium on *compact heat exchangers-history, technological advancement and mechanical design problems*. Book no. G00183, HTD Vol. 10, ASME, New York.

[5]   Cotton, M. A., & Jackson, J. D. (1985). The effect of heat conduction in a tube wall upon forced convection heat transfer in the thermal entry region. In: *Numerical methods in thermal problems*, vol. (iv), Pineridge Press, Swansea, 504-515.

[6]   Peterson, R. B. (1999). Numerical modeling of conduction effects in microscale counter flow heat exchangers. *Microscale Thermophy. Engg.*, **3**, 17-30.

[7]   Maranzana, G., Perry, I., & Maillet, D. (2004). Mini- and micro-channels: influence of axial conduction in the walls. *Int. J. Heat Mass Trans.*, **47**, 3993-4004.

[8]   Li, Z., He, Y. L., Tang, G. H., & Tao, W. Q. (2007). Experimental and numerical studies of liquid flow and heat transfer in microtubes. *Int. J. Heat Mass Trans.*, **50**, 3447-3460.

[9]   Zhang, S. X., He, Y. L., Lauriat, G., & Tao, W. Q. (2010). Numerical studies of simultaneously developing laminar flow and heat transfer in microtubes with thick wall and constant outside wall temperature. *Int. J. Heat Mass Trans.*, **53**, 3977-3989.

[10]   Moharana, M. K., & Khandekar, S. (2012). Optimum Nusselt number for simultaneously developing internal flow under conjugate conditions in a square microchannel. *J. Heat Trans.*, **134**, 071703(01-10).

[11]   Türkakar, G., & Okutucu-Özyurt, T. (2012). Dimensional optimization of microchannel heat sinks with multiple heat sources. *Int. J. Thermal Sciences*, **62**, 85-92.